

ed guides by com-
 this viewpoint the
 image for outcoup-
 than those which
 scale of 30 s.
 f source power, the
 attributed to beam-
 angle was returned
 damage feature as
 ed proportional to
 ed the small spot

it optical damage is
 iLiNbO₃ waveguides
 orders greater than
 experimental condi-
 tions consequences,⁵
 guides in nonlinear
 mixers or parametric

Engineering Research
 an LiNbO₃ Joint

27th October 1986

This transducer can be used for radiating acoustic waves into a medium in contact with the LiNbO₃ surface, as well as into the LiNbO₃ crystal.

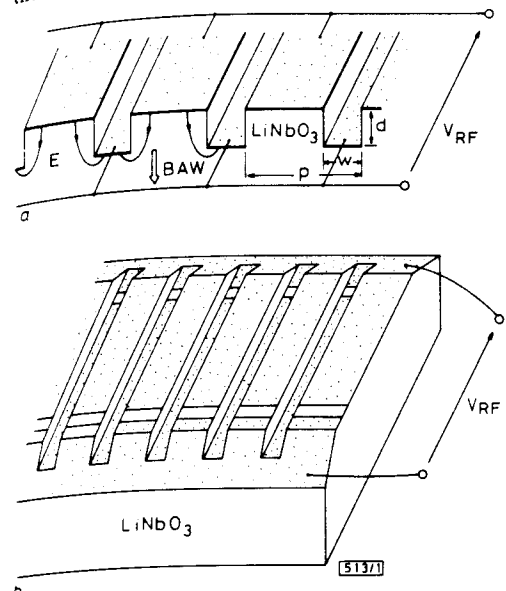


Fig. 1 LiNbO₃ bulk-acoustic-wave transducer
 a Basic structure
 b Practical structure of a relatively low-frequency transducer

If we use ion-etching techniques, grooves with a depth of several micrometres or less would possibly be formed. Thus, it may be possible to obtain a transducer operating at very high frequencies, above several hundred megahertz. Moreover, this transducer is inherently of the nonresonant type, and therefore is expected to have wideband characteristics. Generally, both longitudinal and shear waves can be generated in this structure. The conversion efficiency depends on the surface orientation of the piezoelectric crystal, as well as the configuration parameters, w/d and p/d . As in the case of conventional thickness-mode transducers, the 36°-rotated Y-cut is suitable for longitudinal-wave generation, and the X-cut and the 163°-rotated Y-cut for shear-wave generation.¹ In the case of shear-wave transducers, it is desirable to align the grooves parallel to the displacement vector of the shear wave to be generated.

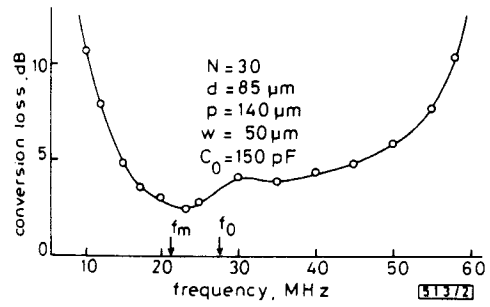


Fig. 2 Conversion loss characteristic of shear-wave transducer using X-cut LiNbO₃

To examine how efficiently bulk waves can be generated in this structure, we fabricated relatively low-frequency transducers. The practical structure is shown schematically in Fig. 1b. The grooves were cut by means of a dicing saw. The electrodes were formed on the top surfaces of the ridges and the bottom face of the grooves by using photolithographic techniques, including a lift-off processing.

First, a shear-wave transducer was fabricated on X-cut LiNbO₃. The grooves were aligned parallel to the displacement of the shear wave, which makes an angle of 37.86° with the crystallographic Z-axis.² The measurements were made by applying an RF pulse signal to the electrodes and observing the echo trains reflecting back from the opposite surface of the plate. The delay time between the echoes agreed well with that

calculated from the shear-wave velocity. The conversion loss CL of the transducer was calculated from

$$CL = \frac{1}{2} \cdot 20 \log_{10} \frac{V_i}{V_0} \text{ dB} \quad (1)$$

where V_0 is the terminal voltage of the 50Ω source generator terminated with a 50Ω load resistance and V_i is the first echo amplitude when the transducer is directly connected to the source generator. The measured conversion loss characteristic is shown in Fig. 2, where N is the number of grooves and C_0 is the clamped capacitance of the transducer. The frequency f_0 where the depth of the grooves is equal to a half-wavelength is indicated in the Figure, along with the frequency f_m where the clamped impedance of the transducer becomes equal to 50Ω. It is seen that the transducer has a large fractional bandwidth of about 110% and a conversion loss as low as 2.5 dB.

Next, we fabricated a longitudinal-wave transducer on 36°-rotated Y-cut LiNbO₃. Fig. 3 shows the measured conversion loss characteristic. This longitudinal-wave transducer also exhibits a broadband characteristic, but the values of the conversion loss are somewhat higher than those of the shear-wave transducer. The cause of the dip seen at 37 MHz in Fig. 3 is not yet satisfactorily understood.

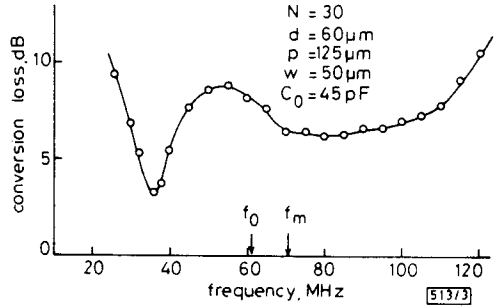


Fig. 3 Conversion loss characteristic of longitudinal-wave transducer using 36° rotated Y-cut LiNbO₃

In conclusion, it has been demonstrated that the multigroove-structure BAW transducers have broadband and efficient conversion characteristics. If ion-etching techniques are used for fabrication of grooves, we may obtain BAW transducers for high frequencies up to several gigahertz. Using this type of BAW transducer, acousto-optic devices, in which LiNbO₃ serves as both the piezoelectric medium for BAW generation and the acousto-optic medium, may be obtained.

K. NAKAMURA
 H. SHIMIZU
 Faculty of Engineering
 Tohoku University
 Aramaki, Sendai, Japan

28th October 1986

References

- 1 WARNER, A. W., ONOE, M., and COQUIN, G. A.: 'Determination of elastic and piezoelectric constants for crystals in class (3m)', *J. Acoust. Soc. Am.*, 1967, **42**, pp. 1223-1231
- 2 WARANABE, A., and YANO, T.: 'Direction of displacement in LiNbO₃ X-cut plate shear transducer', *IEEE Trans.*, 1978, **SU-25**, pp. 159-160

LOW-VOLTAGE MODULATOR AND SELF-BIASED SELF-ELECTRO-OPTIC-EFFECT DEVICE

Indexing terms: Integrated optics, Optical modulators

We have demonstrated a quantum-well waveguide modulator with large (7:1) on/off ratio at low bias voltage (less than 1V) compatible with high-speed electronics. The unique structure of this device permits bistable and other self-electro-optic-effect operations without an external power supply.

There has been much interest in quantum-well (QW) modulators for high-speed fibre-optical communication, as well as integrated optoelectronics. Optical modulators and optical bistable self-electro-optic-effect devices (SEEDs) have been demonstrated at $0.85\ \mu\text{m}$, both in normal incidence^{1,2} and in waveguide geometries.³ An optical modulator has been demonstrated near $1.5\ \mu\text{m}$,⁴ and also a low-voltage integrated laser/modulator device near $0.85\ \mu\text{m}$.⁵ It is important for these applications that the devices be compatible with the low drive voltages of high-speed electronics. We have demonstrated a QW waveguide modulator using the quantum-confined Stark effect (QCSE), which exhibits a large on/off ratio with less than 1 V drive voltage. The unique design of this structure also permits SEED operation without an external power supply. This has applications to integrated optoelectronics.

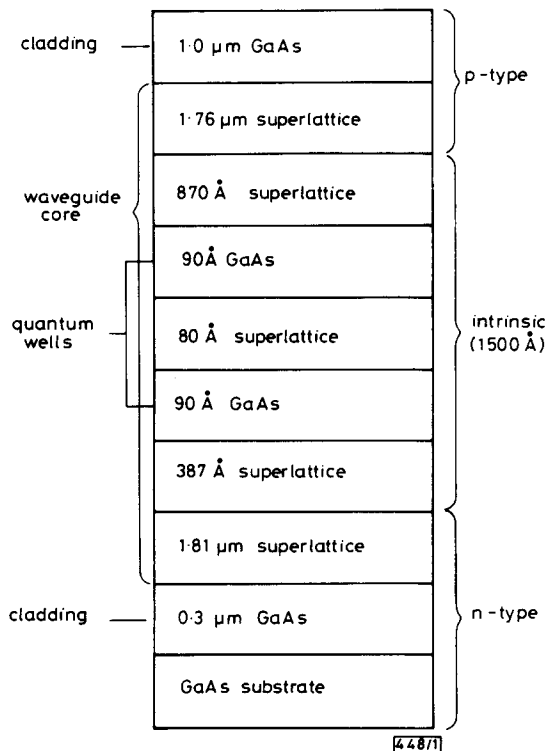


Fig. 1 Sample structure

The superlattice consists of alternate $18\ \text{\AA}$ GaAs and $31\ \text{\AA}$ $\text{Al}_{0.34}\text{Ga}_{0.66}\text{As}$ layers. The n - and p -doping levels are $10^{18}/\text{cm}^3$, except for the top $1000\ \text{\AA}$ of GaAs, which is p -doped to $10^{19}/\text{cm}^3$

The device was grown by molecular beam epitaxy, lattice-matched to a GaAs substrate. The structure (Fig. 1) was similar to that previously used.³ It consisted of two $90\ \text{\AA}$ QWs embedded in a $3.7\ \mu\text{m}$ -thick superlattice (SL) consisting of $18\ \text{\AA}$ GaAs wells and $31\ \text{\AA}$ $\text{Al}_{0.34}\text{Ga}_{0.66}\text{As}$ barriers. The SL is then surrounded by GaAs cladding layers to form a leaky waveguide. As previously explained,³ the design of this structure is crucial to obtaining good contrast ratios. Although the leaky wavelength has nonzero insertion loss, in a real integrated optoelectronic device a conventional waveguide structure could be used, so insertion loss will not be a problem. The structure was PIN-doped to form a diode which could be reverse-biased to apply an electric field to the QWs. In contrast to the previous structure³ the p and n regions are moved much closer to the QW region, giving the much thinner depletion region. The structure was cleaved to $150\ \mu\text{m}$ in length and light from a dye laser was end-fired in to measure the absorption as described in Reference 3.

Fig. 2a and b show the absorption spectra at various voltages for optical electric field \hat{e} parallel and perpendicular to the plane of the layers, respectively. For the \hat{e}_{\parallel} plane, both light hole (lh) and heavy hole (hh) exciton peaks are seen. For the \hat{e}_{\perp} plane only the lh exciton is seen, owing to the selection rules.^{6,7} Because of the narrowness of the intrinsic region, at 0 V the built-in voltage of 1.4 V results in a field of $10^5\ \text{V/cm}$, already enough to shift the absorption to lower energy. Forward-biasing with 0.75 V cancels the built-in field and

causes a 10 meV shift to higher energy. Above 0.75 V forward bias the shift saturates due to current flow. The built-in field is particularly evident in the parallel polarisation spectra of Fig. 2a, in which three absorption peaks are present at zero bias. The highest energy peak is due to the $n = 1$ conduction band to $n = 2$ hh transition, which is forbidden at zero field. This peak disappears when the device is forward-biased.

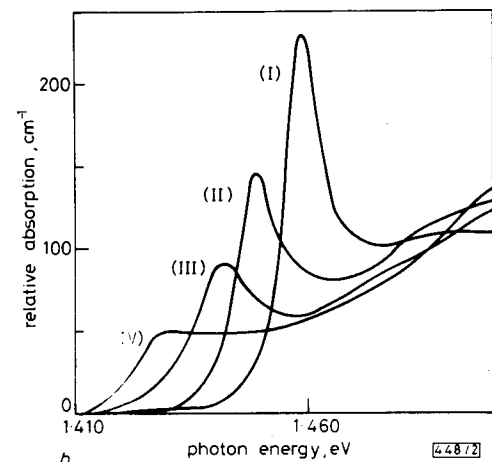
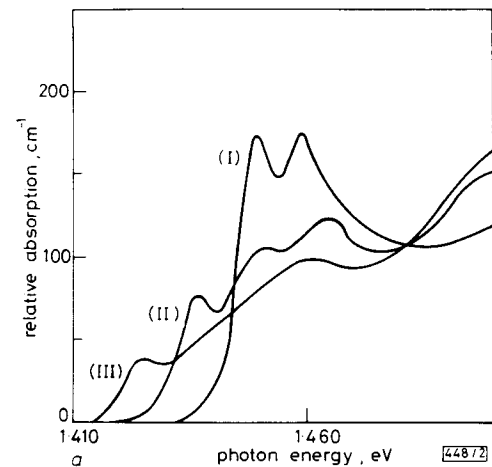


Fig. 2 Absorption spectra of quantum-well modulator for incident polarisation (a) parallel to layers and (b) perpendicular to layers for applied voltages of (i) +0.75 V (ii) 0 V, (iii) -0.5 V, and (iv) -1 V

Positive voltage refers to forward bias

Fig. 3 shows the relative transmission against voltage at $1.447\ \text{eV}$ for the \hat{e}_{\perp} plane. A large on/off ratio of 7:1 is obtained with a forward bias of less than 1 V.

We have demonstrated optical bistability with this device without an external power supply. Here the device is used

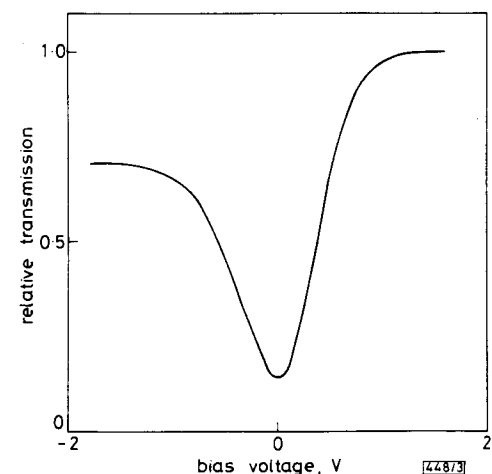


Fig. 3 Relative transmission against voltage for perpendicular polarisation at incident photon energy of $1.447\ \text{eV}$

0.75 V forward
built-in field is
ation spectra of
present at zero
= 1 conduction
den at zero field.
rd-biased.

simultaneously as a modulator and as a detector. The circuit is shown in the inset of Fig. 4. It consists of a photodiode in series with the modulator. A constant light output from a lamp was shone on the photodiode, causing it to act as a constant current source. The laser photon energy was chosen to be that of the zero field exciton peak. With no light the exciton peak is shifted to lower energy by the built-in field. As the incident intensity is increased the photocurrent produced in the modulator increases. When the modulator photocurrent exceeds that of the photodiode it discharges the built-in field, causing the exciton peak to shift towards its zero-field energy and resulting in increased absorption. This results, in turn, in increased modulator photocurrent, and hence, positive feedback and switching. No external voltage is applied. The transfer function of the \hat{e}_\perp plane at an incident photon energy of 1.459 eV is shown in Fig. 4. A large on/off ratio of 7:1 is obtained. This could be increased by adding more QWs or by increasing the length of the device. We note that other SEED operations such as optical level shifting and self-linearised modulation² will work in this configuration.

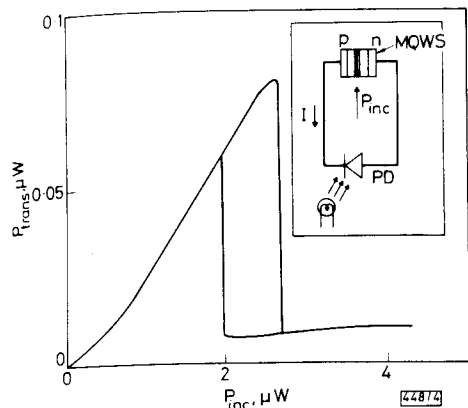


Fig. 4 Measured transfer characteristic at 1.459 eV incident photon energy using circuit shown in inset

The incident optical polarisation was perpendicular to the layers

We also point out that by reducing the thickness of the intrinsic region still further, it should be possible to make the built-in field large enough to obtain optical bistability with the photodiode replaced with a resistive load.†

In conclusion, we have demonstrated a low-voltage QCSE optical modulator compatible with high-speed electronics. With this device we have demonstrated SEED optical bistability without the use of an external power supply. This device has potential application to high-speed optoelectronics and optical switching devices.

We are pleased to acknowledge the assistance of J. E. Henry in sample preparation.

J. S. WEINER
A. C. GOSSARD
J. H. ENGLISH

AT&T Bell Laboratories
Murray Hill, NJ 07974, USA

D. A. B. MILLER
D. S. CHEMLA

AT&T Bell Laboratories
Holmdel, NJ 07733, USA

C. A. BURRUS

AT&T Bell Laboratories
Crawford Hill Laboratory
Holmdel, NJ 07733, USA

References

- MILLER, D. A. B., CHEMLA, D. S., DAMEN, T. C., GOSSARD, A. C., WIEGMANN, W., WOOD, T. H., and BURRUS, C. A.: 'Band-edge electro-

† In general, optical bistability is easier to obtain as the voltage and/or series resistance are increased. The photodiode acts as a constant current source, which is equivalent to an infinite voltage and resistance, and hence produces optical bistability at a lower voltage than the resistor. For a detailed discussion of this point see Reference 2

- absorption in quantum well structures: the quantum confined Stark effect'. *Phys. Rev. Lett.*, 1984, **53**, pp. 2173-2176
- MILLER, D. A. B., CHEMLA, D. S., DAMEN, T. C., WOOD, T. H., BURRUS, C. A., GOSSARD, A. C., and WIEGMANN, W.: 'The quantum well self electrooptic effect device: optoelectronic bistability and oscillation, and self-linearized modulation', *IEEE J. Quantum Electron.*, 1985, **QE-21**, pp. 1462-1476
- WEINER, J. S., MILLER, D. A. B., CHEMLA, D. S., DAMEN, T. C., BURRUS, C. A., WOOD, T. H., GOSSARD, A. C., and WIEGMANN, W.: 'Strong polarization sensitive electroabsorption in GaAs/AlGaAs quantum well waveguides', *Appl. Phys. Lett.*, 1985, **47**, pp. 1148-1150
- WAKITA, H., KAWAMURA, Y., YOSHIKUNI, Y., and ASAHI, H.: 'High temperature excitons and enhanced electroabsorption in InGaAs/InAlAs multiple quantum wells'. *Electron. Lett.*, 1985, **21**, pp. 574-576
- TARUCHA, S., and OKAMOTO, H.: 'Monolithic integration of a laser diode and an optical waveguide modulator having a GaAs/AlGaAs quantum well double heterostructure', *Appl. Phys. Lett.*, 1985, **48**, pp. 1-3
- ARAKAWA, Y., LARSON, A., PASLASKI, J., and YARIV, A.: 'Active switching in a GaAs/AlGaAs multiquantum well laser with an intracavity monolithic loss modulator', *ibid.*, 1986, **48**, pp. 561-563
- WEINER, J. S., CHEMLA, D. S., MILLER, D. A. B., HAUS, H. A., GOSSARD, A. C., WIEGMANN, W., and BURRUS, C. A.: 'Highly anisotropic optical properties of single quantum well waveguides', *ibid.*, 1985, **47**, pp. 664-667

VERY HIGH-TRANSCONDUCTANCE HETEROJUNCTION FIELD-EFFECT TRANSISTOR (HFET)

Indexing terms: Semiconductor devices and materials, Field-effect transistors

A new form of FET has been demonstrated in the GaAs/AlGaAs material system. Designated the HFET, it has shown a transconductance of 500 mS/mm at 300 K for a nominal $L_g = 2 \mu\text{m}$ and a drain current of 430 mA/mm. The conduction occurs in an inversion channel at the heterointerface.

The sustained interest in heterojunction FETs over the last few years has been fuelled by the demand for a device structure fabricated in a high-mobility (and high-drift-velocity) material system and suitable as the basis for a VLSI technology. Most of the effort has focused on the HEMT¹⁻⁴ (high-electron-mobility transistor), and many variations of the device have been investigated including normal and inverted structures, self-aligned and non-self-aligned devices and those that incorporate pseudomorphic strained layers to achieve higher channel mobilities. More recently the SISFET⁵ (semiconductor-insulator-semiconductor FET) has been investigated because of the way in which it closely emulates the MOSFET, the highly successful base of silicon VLSI technology.

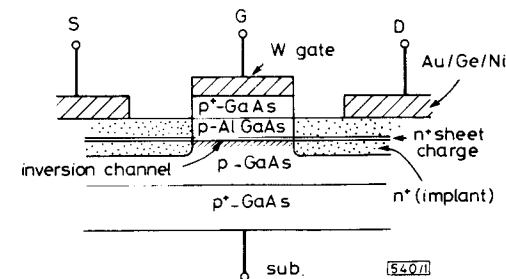


Fig. 1 Physical cross-section of HFET

Although many of these structures hold promise in terms of individual device performance, it is still unclear that they can meet the requirements of uniformity and reproducibility that are necessary for a VLSI technology. In the search for alternative means to achieve a uniform and precisely controlled

tor for incident pol-
to layers for applied
-1V

gainst voltage at
ratio of 7:1 is

with this device
ne device is used

perpendicular polarisa-